



HIGHLY ADAPTABLE RUBBER ISOLATION SYSTEMS

**Luis DORFMANN¹, Maria Gabriella CASTELLANO²,
Stefan L. BURTSCHER³, Donatella CHIAROTTO⁴**

SUMMARY

Elastomeric bearings used in seismic isolation of structures are traditionally built with an in-plane isotropic layout by vulcanization bonding of sheets of rubber to thin reinforcing plates. The bearings are assembled alternating horizontal and flat layers of rubber and steel plates. Their behavior in shear is therefore equal in any in-plane direction.

The objective of this paper is to describe the mechanical characteristics of elastomeric bearings with different shear stiffness along the two principal in-plane directions. This can be useful for seismic protection of structures with very distinct dynamic characteristics in two directions, such as bridges and viaducts. The different shear stiffness along the two principal in-plane directions is accomplished by arranging all steel reinforcing plates to be V-shaped, forming an angle α with respect to the horizontal plane. The slope of the V-shaped plates is positive in the first part of the bearing and changes sign in the second part. Fourteen prototypes have been manufactured with seven different layouts, with different angle - in the range from 3° to 7° - and different shape factor. One of these bearings has a conventional design with horizontal steel laminae, which serves as our baseline case.

The bearings are subjected to a series of compression and shear tests. The results are summarized and compared. It is shown that the new concept provides a valuable design alternative for elastomeric isolators. The generated stiffness of the new design is different in the two principal in-plane directions. The stiffness ratio can be varied as a design quantity to maximize the benefit provided by laminated elastomeric bearings in seismic isolation of structures.

The results of numerical analyses show clearly that it is important to include stress softening attributed to cavitation in the numerical characterization of said elastomeric bearings.

¹ Dr., Institute of Structural Engineering, Peter Jordan Str. 82, 1190 Vienna, Austria, dorfmann@mail.boku.ac.at

² Dr., Research Engineer, R&D Dep., FIP Industriale, Selvazzano Dentro, Italy, castellano.fip@fip-group.it

³ Dr., Institute of Structural Concrete, Technical University of Vienna, stefan.burtscher@tuwien.ac.at

⁴ President and CEO, FIP Industriale, Selvazzano Dentro, Italy, chiarottod.fip@fip-group.it

INTRODUCTION

Seismic isolation is a well-known method, which is in general preferred over the more traditional method of strengthening of structural components. Amongst the many types of seismic isolation devices proposed over the last 30 years, elastomeric isolators are the primary choice throughout the world, in particular for base isolation of buildings (Skinner [1], Kelly [2]). They are built by vulcanization bonding of sheets of rubber to thin steel reinforcing plates. The reinforcing plates constrain the elastomer from lateral expansion and provide therefore a very high vertical and bending stiffness, but do not affect the high flexibility in the horizontal direction. Typically, the shear stiffness can be two or three order of magnitude smaller than the vertical stiffness. The reinforcing steel plates are horizontal, thus the shear behavior is equal in any in-plane direction.

The objective of this study is to evaluate the mechanical characteristics of elastomeric bearings with different shear stiffness in two principal in-plane directions. This is accomplished by arranging all steel reinforcing plates to form an angle α with respect to the horizontal plane. The slope of the V-shaped plates is positive in the first part of the bearing and changes sign in the second part. The direction in which the steel plates are V-shaped is defined transversal having in mind the position of the isolator under a bridge. In the orthogonal horizontal direction, i.e. the longitudinal direction, the cross section of the isolator does not change, thus the shear behavior in this direction is expected to be equal to that of a conventional isolator with the same geometry but flat steel plates. The V-shaped isolators have been denominated as “Highly Adaptable Rubber Isolation Systems (HARIS)”, to focus on the fact that the bearing layout can be customized to obtain different shear stiffness in two orthogonal directions.

The behavior of HARIS was verified experimentally as well as by a series of numerical analyses, which are described in part in this paper.

PROTOTYPES LAYOUT AND TESTING PROGRAM

Haris Prototype bearings may be subdivided into 7 different layouts. They were manufactured and used for static as well as dynamic tests performed at the laboratories of Institute of Structural Engineering and of FIP Industriale, respectively. All bearings have a 200 mm x 200 mm external cross sectional dimension, while the internal steel shims are 195 mm x 195 mm with a thickness of 2 mm each. The remaining geometric dimensions differ for each layout and are summarized in Table 1. Different geometric parameters are selected to experimentally evaluate the influence of shape factor as well as the shape of the steel plates (V-shaped or cylindrically shaped) and the slope of the V-shaped reinforcements on the isolator behavior. A graphical summary of the seven layouts is produced in Figure 1.

The geometric layouts differ in the shape factor S ($S = \text{loaded area} / \text{force-free area of each rubber layer}$) and in the inclination of the V-shaped steel laminae. There are three different values of the shape factor for bearings of a rubber layer of 2 mm, 4 mm and 6 mm, which correspond to a shape factor $S=24.4$, 12.2 and 8.1, respectively. Furthermore, the bearing design includes a slope α of 3° , 5° and 7° for reinforcing steel plates. In addition, Haris 02 has cylindrical shaped steel plates with a radius of curvature equal to 575 mm, which corresponds to an equivalent slope of 5° . The use of V-shaped steel plates seems preferable from a manufacturing standpoint, whereas cylindrical steel plates might be preferable to avoid stress concentration. The Haris 02 prototype bearing is thus aimed to verify whether this plate layout versus the V-shape layout lends the devices a better total performance, particularly in terms of failure limit. One layout (Haris 07) has flat ($\alpha=0^\circ$) steel plates, and serves as our reference prototype.

Table 1 - Geometric Characteristics of Prototypes for Static and Dynamic Tests.
 (*=cylindrical shaped plates with a 575 mm radius).

Bearing type	Skew Angle	Thickness of each rubber layer (mm)	Number of rubber layers
Haris 01	5	4	10
Haris 02	(*)	4	10
Haris 03	5	2	20
Haris 04	5	6	7
Haris 05	3	4	10
Haris 06	7	4	10
Haris 07	0	4	10

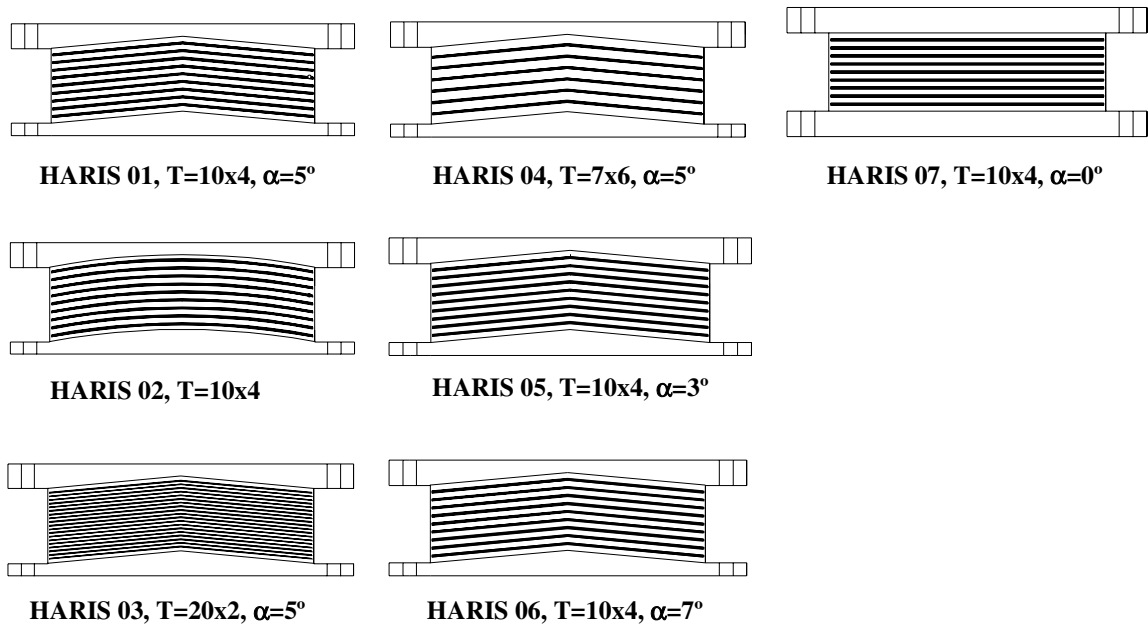


Figure 1 - Geometric Layout of Prototypes for Static and Dynamic Tests.

Static compression and static and dynamic shear tests are performed to characterize each bearing under constant design compressive load (6 MPa) and shear displacements (at increasing shear strain up to failure). Shear modulus and damping are evaluated as a function of shear strain. Two compression tests, aimed at measuring the axial stiffness, are carried out, up to an average compressive stress of 6 and 10 MPa, respectively. During all shear tests the vertical load is maintained constant at 6 MPa. Dynamic shear tests are carried out at a frequency of 0.5 Hz, that is a typical frequency of an isolated structure, and thus considered as the reference testing frequency by many standards or guidelines. Dynamic shear tests are carried out at the following values of shear strain: 10 %, 20 %, 50 %, 100 % and 150 %. Shear tests at

higher shear strains are carried out or at a lower frequency (0.3 Hz) or at constant velocity, equal to 150 mm/min, due to power limitations. Two cycles are carried out for compression tests, whereby the vertical stiffness is determined during the second cycle. Three cycles are carried out for shear tests, and the stiffness is determined for the third cycle. All shear tests are carried out on a pair of identical bearings as shown in Figure 2. Thus, recorded readings are for the combination of two bearings; shear loads in each bearing are half the value shown.

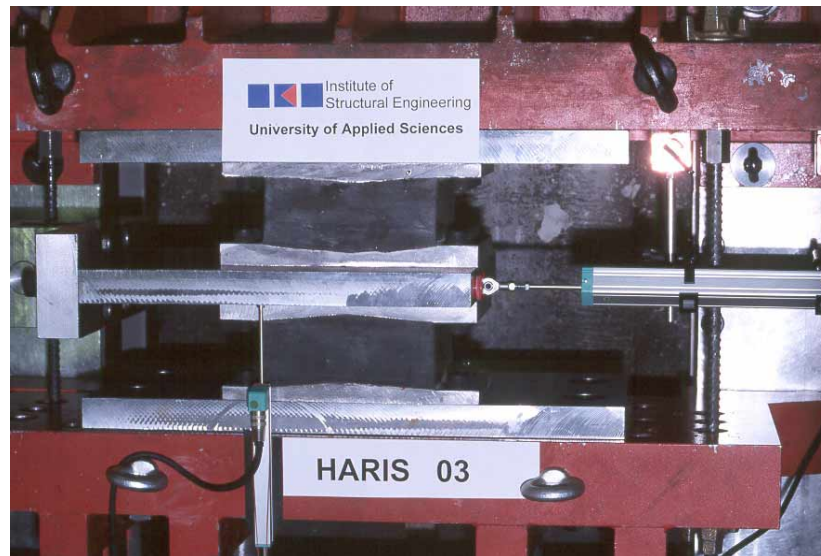


Figure 2 – A couple of prototypes under testing.

TEST RESULTS

No significant differences are found during compressive tests on different layout's isolators, therefore no compression results are shown here.

Some shear tests have been carried out both in transversal and longitudinal horizontal direction on V-shaped prototypes. Test results confirm that the shear behavior in longitudinal direction is the same as the shear behavior of reference prototype Haris 07 with flat steel plates. Therefore, in the following the shear behavior in the transversal direction only is described and compared with the behavior of reference prototype.

First, isolators with the same number and thickness of rubber layers (i.e. same shape factor) but different skew angles are compared. As expected the isolators with a higher skew angle are substantially stiffer in transverse direction (direction of the V-shaped laminae and testing direction) for up to about 40 mm displacement, i.e. 100 % shear strain (s.s.), see Figures 3 and 4. The bearing Haris 01 ($\alpha=5^\circ$) provides, for example, a maximum force at 100 % shear strain, which is about 170 % higher than the force of reference bearing Haris 07. It can be observed that in V-shaped isolators the force vs. displacement behavior is highly nonlinear compared to the reference bearing Haris 07. By increasing the angle α , the non-linearity increases as well. In Figure 5, the bearing with cylindrical steel plates is compared to Haris 01 ($\alpha=5^\circ$); no substantial differences are noted, even at higher shear strain. Therefore, it can be concluded that the V-shape layout is almost equivalent to the cylindrical design. There are no big differences between the static and dynamic shear behavior.

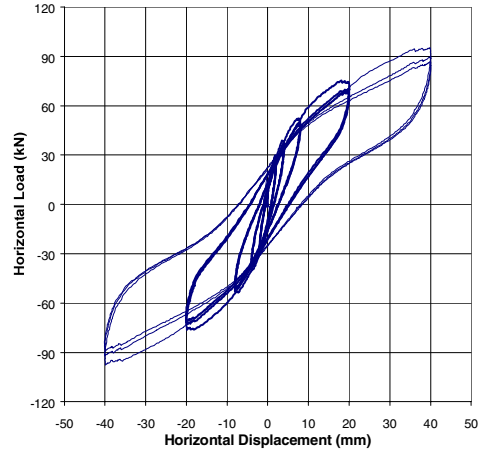
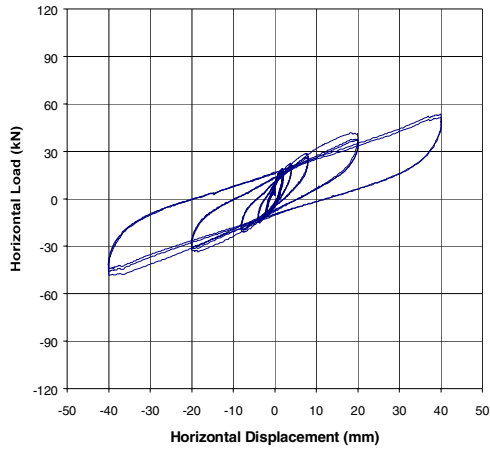


Figure 3 - Static Shear Test at 100% s.s. for Haris 07 (10x4mm, 0°), Haris 01 (10x4mm, 5°).

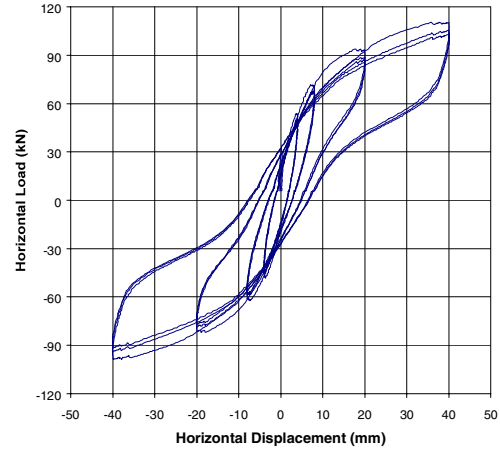
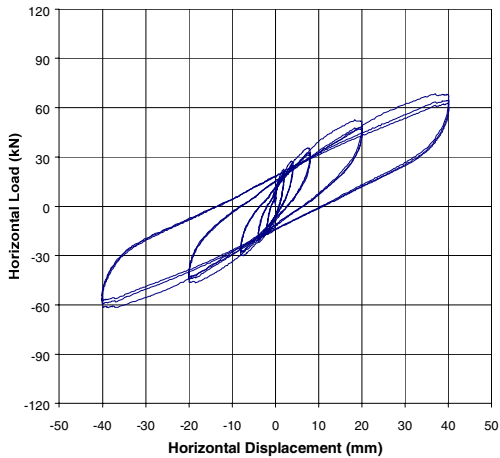


Figure 4 - Static Shear Test at 100% s.s. for Haris 05 (10 x 4mm, 3°), Haris 06 (10 x 4mm, 7°).

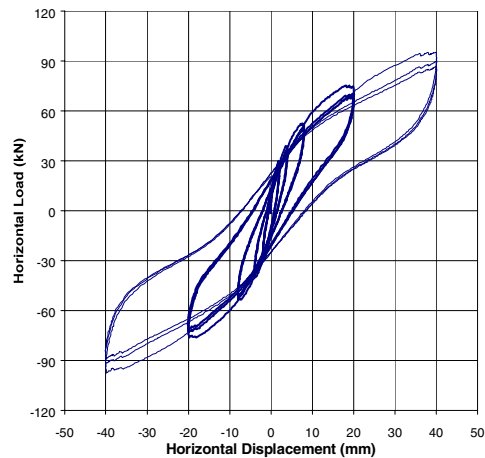
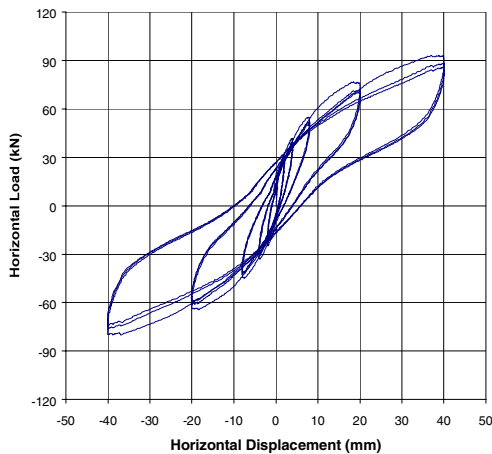


Figure 5 - Static Shear Test at 100% s.s. for Haris 02 (R=575mm, 5°), Haris 01 (10 x 4mm, 5°)

For shear strains above 100 % the interpretation of the test data is not straightforward any longer, see Figure 6, which shows the equivalent dynamic shear modulus G versus shear strain for prototypes having the same shape factor. The ratio of the shear moduli of different bearings over the shear modulus of the

reference bearing Haris 7 (0°) is shown in Figure 7 as a function of the shear strain. Up to shear strains of about 100 % the trend is quite clear: higher skew angle translates into higher shear stiffness ratio. At higher shear strain, the difference for different layouts decrease, and at shear strains higher than 200 % the stiffness ratio becomes approximately equal to 1. This is deemed due, at least in part, to the fact that the steel laminae are subjected to bending deformation and the original angle of inclination changes as shown in Figure 8. For flat geometry the deformation in each individual rubber layer is simple shear. In the V-shaped layout, the state of deformation is a combination of hydrostatic compression and tension as well as shear.

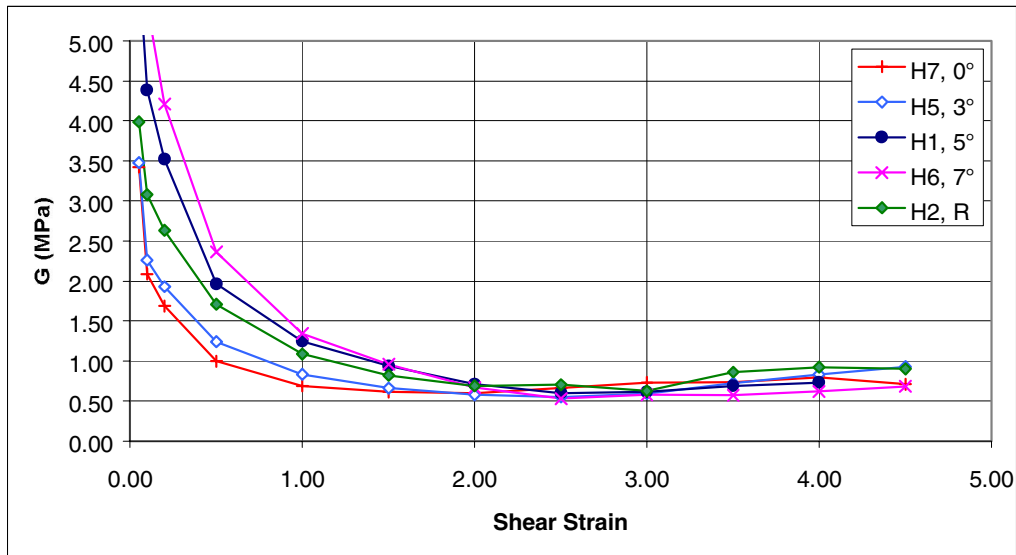


Figure 6 – Dynamic shear modulus versus shear strain for different skew angles (isolators with the same shape factor).

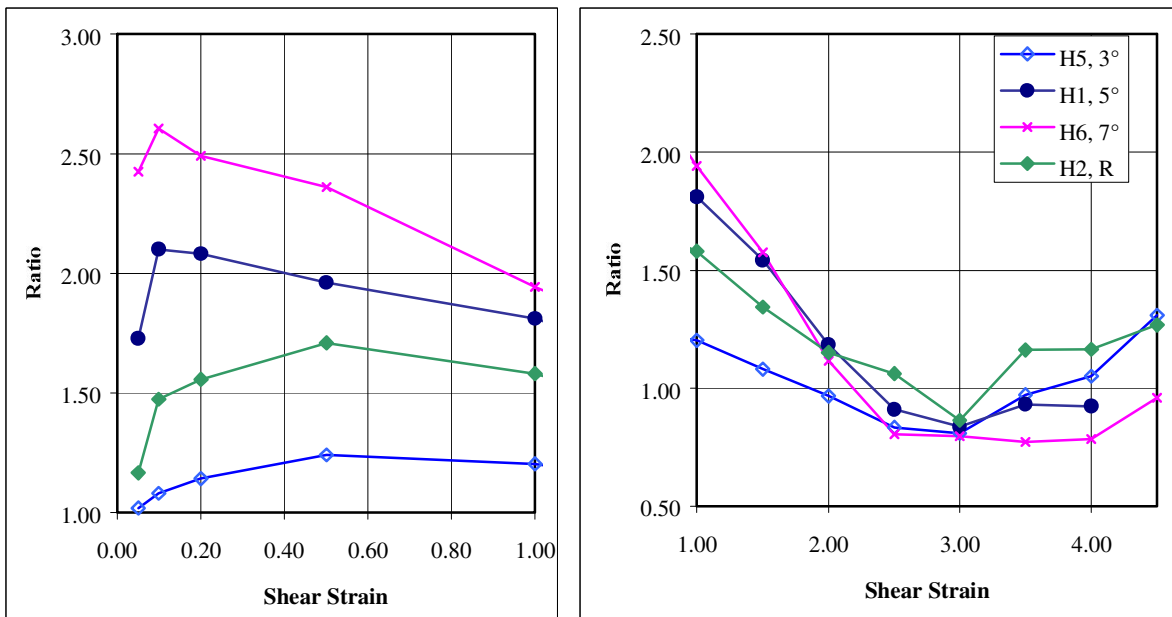


Figure 7 – Ratio of dynamic shear modulus of Haris bearings with Haris 7 (0°).



Figure 8 – Bending deformation of steel plates subjected to high shear strains.

Finally, the influence of the shape factor is shown in Figure 9 and Figure 10. Haris 01, Haris 03 and Haris 04 all have a skew angle of 5° and approximately the same overall height, but a different number and a different thickness of rubber layers. It can be seen that by increasing the thickness of individual rubber layers (decreasing the shape factor), the bearings become more flexible, and the inclination of the steel plates becomes much less effective in increasing the shear stiffness. In effect, at 100 % shear strain the shear stiffness of Haris 04 is only 1.25 times the shear stiffness of Haris 07 at the same shear strain.

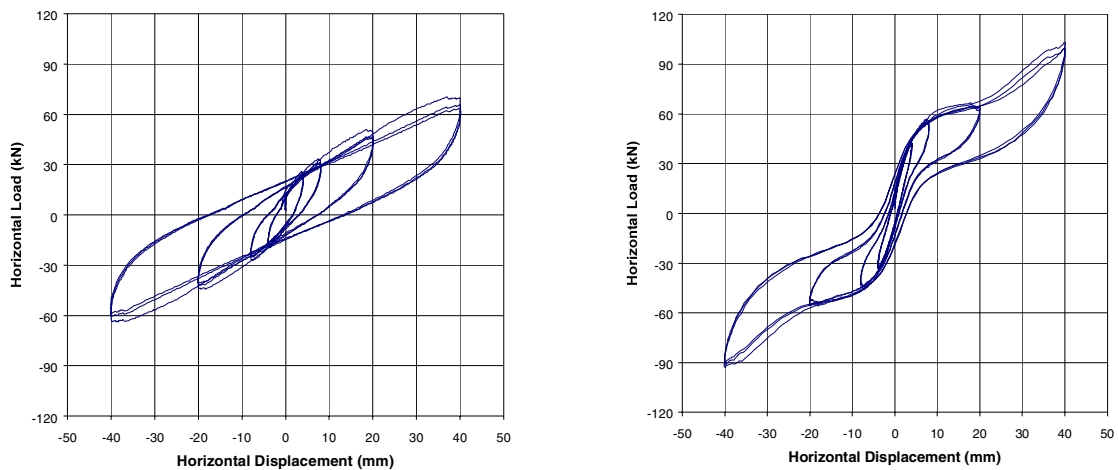


Figure 9 - Static Shear Test at 100% s.s. for Haris 04 (7 x 6mm, 5°), Haris 03 (20 x 2mm, 5°).

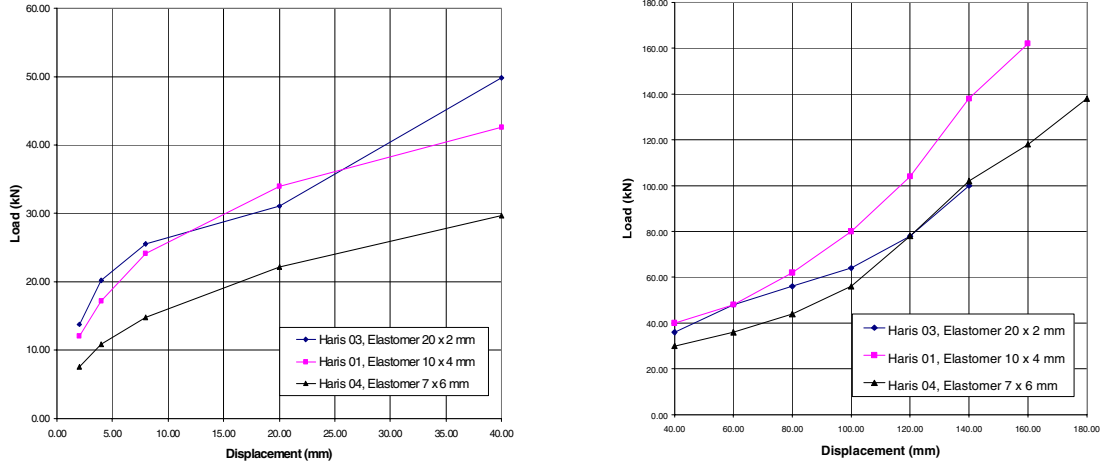


Figure 10 - Maximum Horizontal Load vs. Shear Displacement for HARIS Prototypes with the same skew angle (5°) and different shape factors (static tests).

As far as the displacements at failure, the tests gave very satisfactory results for all prototypes. In fact, shear failure occurred at shear strain higher than 400 %, except for Haris 3, which failed at a shear strain of 375 %. The failure mechanism was for all prototypes a shear failure in rubber and not a loss of adhesion between rubber and steel plates.

STRESS SOFTENING MODEL

For full details of the relevant theory of elasticity summarized in this section we refer to, for example Ogden [3].

We consider first a multiplicative decomposition of the deformation gradient \mathbf{F} into a volume-changing (dilatational) and a volume-preserving (isochoric) part in the form

$$\mathbf{F} = (J^{1/3} \mathbf{I}) \bar{\mathbf{F}} = J^{1/3} \bar{\mathbf{F}} \quad (1)$$

following Flory [4] and Ogden [5, 3] The modified deformation tensor $\bar{\mathbf{F}}$ describes the volume-preserving part of the deformation, while the dilatational part is given in terms of the determinant $J = \det \mathbf{F}$. It follows from equation (1) that

$$\det \bar{\mathbf{F}} = 1. \quad (2)$$

We denote by λ_i , $i = 1, 2, 3$, the principal stretches of the deformation and the modified principal stretches $\bar{\lambda}_i$, $i = 1, 2, 3$ are defined by

$$\bar{\lambda}_i = J^{-1/3} \lambda_i. \quad (3)$$

It follows that

$$\bar{\lambda}_1 \bar{\lambda}_2 \bar{\lambda}_3 = 1. \quad (4)$$

Here, we consider the material to be isotropic and elastic, so that the strain-energy function is a symmetric function, $W(\lambda_1, \lambda_2, \lambda_3)$ say, of the principal stretches.

In order to separate the dependence of W into the isochoric and dilatational parts of the deformations, we regard it as a function of $\bar{\lambda}_1, \bar{\lambda}_2, \bar{\lambda}_3$ and J subject to (4), and we write

$$\bar{W}(\bar{\lambda}_1, \bar{\lambda}_2, \bar{\lambda}_3, J) = W(\bar{\lambda}_1 J^{1/3}, \bar{\lambda}_2 J^{1/3}, \bar{\lambda}_3 J^{1/3}), \quad (5)$$

which defines the notation \bar{W} . The principal Cauchy stresses σ_i are then given by

$$J\sigma_i = \bar{\lambda}_i \frac{\partial \bar{W}}{\partial \bar{\lambda}_i} - \bar{p}, \quad (6)$$

where \bar{p} is defined by

$$\bar{p} = \frac{1}{3} \sum_{j=1}^3 \bar{\lambda}_j \frac{\partial \bar{W}}{\partial \bar{\lambda}_j} - J \frac{\partial \bar{W}}{\partial J}. \quad (7)$$

The hydrostatic part of the stress is given simply by

$$\frac{1}{3}(\sigma_1 + \sigma_2 + \sigma_3) = \frac{\partial \bar{W}}{\partial J} \quad (8)$$

For the special case in which W is decoupled into dilatational and volume-preserving parts we write

$$W(\lambda_1, \lambda_2, \lambda_3) = W(\bar{\lambda}_1, \bar{\lambda}_2, \bar{\lambda}_3, J) = W_{\text{vol}}(J) + W_{\text{iso}}(\bar{\lambda}_1, \bar{\lambda}_2, \bar{\lambda}_3), \quad (9)$$

where $W_{\text{vol}}(J)$ and $W_{\text{iso}}(\bar{\lambda}_1, \bar{\lambda}_2, \bar{\lambda}_3)$ respectively are the volumetric and volume-preserving parts of the energy.

Over the last decades extensive research has been conducted into the development of constitutive laws for both incompressible and compressible elastic materials, but to the best of the authors' knowledge there is no formulation currently available in the literature that accounts for the nonlinear tension-volume response due to cavitation. This may be due to the assumption of incompressibility frequently used for the analysis of rubber. However, experimental evidence discussed by Dorfmann et al. [6] and Dorfmann [7] indicates clearly that incompressibility is not appropriate, and, when the material is subject to hydrostatic tensions beyond a critical value, neither is a linear tension-volume response.

We propose first to derive an expression for the volumetric part W_{vol} of the strain energy, the first derivative of which gives the hydrostatic pressure in accordance with equation (8). The second derivative is the bulk modulus. For an increase in volume ($J > 1$) it is important that the strain energy function takes into account the growth of microcavities and fracture of weak junctions in polymer chains.

The choice of the function $W_{\text{vol}}(J)$ is arbitrary, subject to the usual requirements that it has an absolute minimum at $J = 1$ and that its first derivative gives the hydrostatic tension-volume response. To describe the pressure-volume relation during the initial loading process, we propose to use the tangent hyperbolic function with two material parameters m and κ such that the dilatational strain energy can be expressed as

$$W_{\text{vol}}(J) = m\kappa \int_1^J \tanh \left[\frac{1}{m}(J-1) \right] dJ, \quad (10)$$

where κ is the bulk modulus for the material in the natural configuration before any damage occurs. The pressure-volume relation is then given by

$$p(J) = m \kappa \tanh \left[\frac{1}{m} (J - 1) \right]. \quad (11)$$

The parameter m provides enough flexibility to enable the bulk modulus to be changed gradually from its initial value κ to essentially zero.

NUMERICAL CHARACTERIZATION OF SEISMIC ISOLATORS

The numerical determination of the shear stiffness and the pressure distribution of the bearing shown in Figure 8 is attempted. The deviatoric strain energy contribution W_{iso} is given by the Ogden energy formulation in principal stretches [5], while for the dilatational contribution to the strain energy the above described stress softening model, taking into account rubber cavitation, is suggested. Thus the complete strain energy formulation for hyperelastic materials is now given by

$$W = \sum_{i=1}^3 \frac{2\mu_i}{\alpha_i^2} \left(\bar{\lambda}_1^{\alpha_i} + \bar{\lambda}_2^{\alpha_i} + \bar{\lambda}_3^{\alpha_i} - 3 \right) + m \kappa \int_1^J \tanh \left[\frac{1}{m} (J - 1) \right] dJ \quad (12)$$

Results of the numerical model are compared to the experimental data in Figure 11. The accuracy of the numerical results show clearly that it is important to include stress softening attributed to cavitation in the numerical characterization of Haris bearings. It is shown that the solution with no cavitation is too stiff and does not reproduce experimental data.

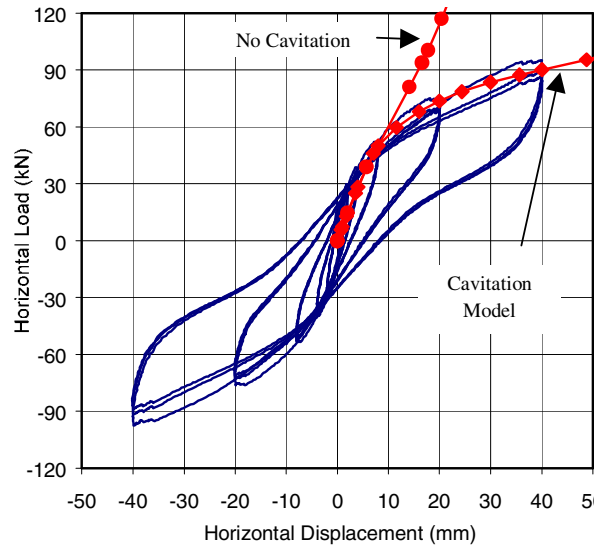


Figure 11 - Numerical and experimental load-displacement response for bearings with inclined steel plates (Skew angle of 5°, Haris 01)

CONCLUSIONS

Elastomeric bearings based on an alternative design concept have been built and tested. The new design consists of V-shaped or cylindrical-shaped steel plates. To validate this concept, isolators with seven different layouts were tested. The results are summarized in this paper; it is shown that the new concept

provides a valuable design alternative for elastomeric isolators. The generated shear stiffness of the new design is different in the two principal in-plane directions, as desired. The parametric tests have shown the effect of different geometric parameters on the ratio of the stiffness values in the two directions. Maximum value of the stiffness ratio obtained in these tests at 100 % shear strain is close to two. This ratio can be varied and used as a design quantity to maximize the benefit provided by laminated elastomeric bearings in seismic isolation of structures. The behaviour of said bearings can be reproduced by numerical analyses that include stress softening attributed to cavitation of the elastomer.

ACKNOWLEDGMENTS

Support for this research was provided by the European Commission, as part of the research program “Highly Adaptable Rubber Isolating Systems (HARIS)”, Contract No. BRPR-CT95-0072, Project No. BE-1258. This support is gratefully acknowledged.

REFERENCES

1. Skinner, R.I., Robinson, W.H., McVerry, G.H. “An Introduction to Seismic Isolation”, John Wiley & Sons Ltd. 1996.
2. Kelly, J.M. “Earthquake-Resistant Design with Rubber”, Springer Verlag, 1997.
3. Ogden, R.W. “Non-linear Elastic Deformations”, New York: Dover 1997.
4. Flory R. W. “Thermodynamic Relations for High Elastic Materials”, *Trans. Faraday. Soc.* 57, 829-838, 1961.
5. Ogden R.W. “Large Deformation Isotropic Elasticity: On the Correlation of Theory and Experiments for Incompressible Rubberlike Solids”, *Royal Society of London A* 328, 567-583, 1972.
6. Dorfmann A., Fuller K.N.G., Ogden R.W. “Shear, compressive and dilatational response of rubberlike solids subject to cavitation damage”, *International Journal of Solids and Structures* 39, 1845-1861, 2002.
7. Dorfmann A. “Stress Softening of Elastomers in Hydrostatic Tension”, *Acta Mechanica*, 165, 117-137, 2003.